Ray tracing in the smoothed acoustic SEG/EAGE Salt Model. Part 2: Maps of reflections

Václav Bucha

Department of Geophysics, Faculty of Mathematics and Physics, Charles University, Ke Karlovu 3, 121 16 Praha 2, Czech Republic, E-mail: bucha@seis.karlov.mff.cuni.cz

Summary

Two-point rays of the P-wave reflected from the flat bottom interface in the smoothed acoustic SEG/EAGE Salt Model are calculated. The shot-receiver configurations are derived from the original SEG/EAGE Phase A Acquisition. Reflection points are used for generating reflection maps, colour coded according to amplitudes. The illumination of the large shadow area below the trunk of the salt body is discussed.

Keywords

Velocity model, ray tracing, seismic waves, maps of reflections

1 Introduction

The first part of this article (Bucha 2006) presented the calculation of two-point rays and the generation of ray theory seismograms in the smoothed acoustic SEG/EAGE Salt Model. This second part of the article is devoted to computing two-point rays and to constructing maps of reflections in the same model.

We are interested in finding the reflectors below the salt bodies. The high-velocity contrast and various complex shapes of the salt bodies create shadow zones below the salt where little energy is reflected. Ray tracing is the method used to model and study these situations with respect to real field seismic measurements (Bear et al. 2000, Muerdter et al. 2001abc).

This article describes the construction of reflection maps in the smoothed acoustic SEG/EAGE Salt Model. To study the subsalt area, two-point rays of P-waves reflected from the bottom flat interface for selected shot-receiver configurations are computed. Reflection points, colour coded according to amplitudes, are generated and plotted.

The GOCAD program was used to visualize the 3-D smoothed Salt Model with interfaces, shots, receivers, computed two-point rays and maps of reflections. All computations were performed on a PC with the Linux operating system.

Submitted for publication in: *Journal of Seismic Exploration.* In: Seismic Waves in Complex 3-D Structures, Report 16 (Department of Geophysics, Charles University, Prague, 2006), pp. 17–28

2 Smoothed acoustic SEG/EAGE Salt Model

The Salt Model selected for ray tracing computations was smoothed by Bulant (2001, 2002, 2004). It is the best model obtained as a result of many test smoothing computations. The model is parameterized by B-splines and was smoothed using Sobolev scalar products. The smoothed Salt Model is composed of the most important interfaces and velocity blocks. The interfaces, which are characterized by the highest discontinuities in the velocity field, are the ocean bottom, the interfaces limiting the salt body, the geopressure horizon and the bottom flat interface (see Figure 1). The velocity blocks are the water (velocity is constant), the background above the geopressure horizon (three-dimensionally varying velocity), the salt (velocity is constant), the background below the geopressure horizon (three-dimensionally varying velocity) and the bottom half-space (velocity is constant).

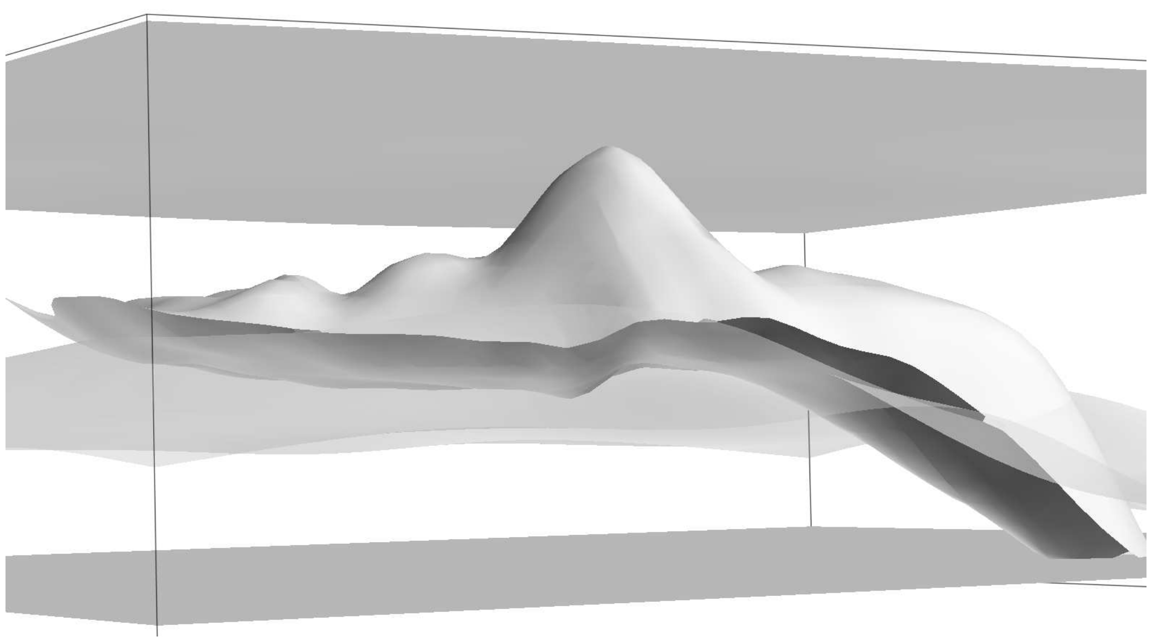

Figure 1. Detailed view of the salt body in the smoothed Salt Model. The most important interfaces are: the ocean bottom, the interfaces limiting the salt body, the geopressure horizon, the bottom flat interface. The geopressure horizon is partially transparent.

3 Shots and receivers

The position of the shots and receivers is derived from the original SEG/EAGE Phase A Acquisition (Aminzadeh, Brac & Kunz, 1997). Figures 2 and 3 show six shot-receiver configurations used to calculate the two-point rays.

The basic configuration is the square of 21x21 receivers with the centre above the crest of the salt (configurations M2 and M5 on Figure 2). The square of receivers and sources is shifted by half of the square side to the right, left and towards the top of the paper (see Figures 2 and 3). The shift of receivers towards the bottom of the paper was smaller than half of the square side because of the boundary of the model. The receivers are located at a depth of 0 m and the grid step is 320 m. There are 9 shots for each configuration with one exception for the central configuration M5 with only 8 shots (the central shot is not duplicated). The shots are located at a depth of 20 m and at steps of 800 m.

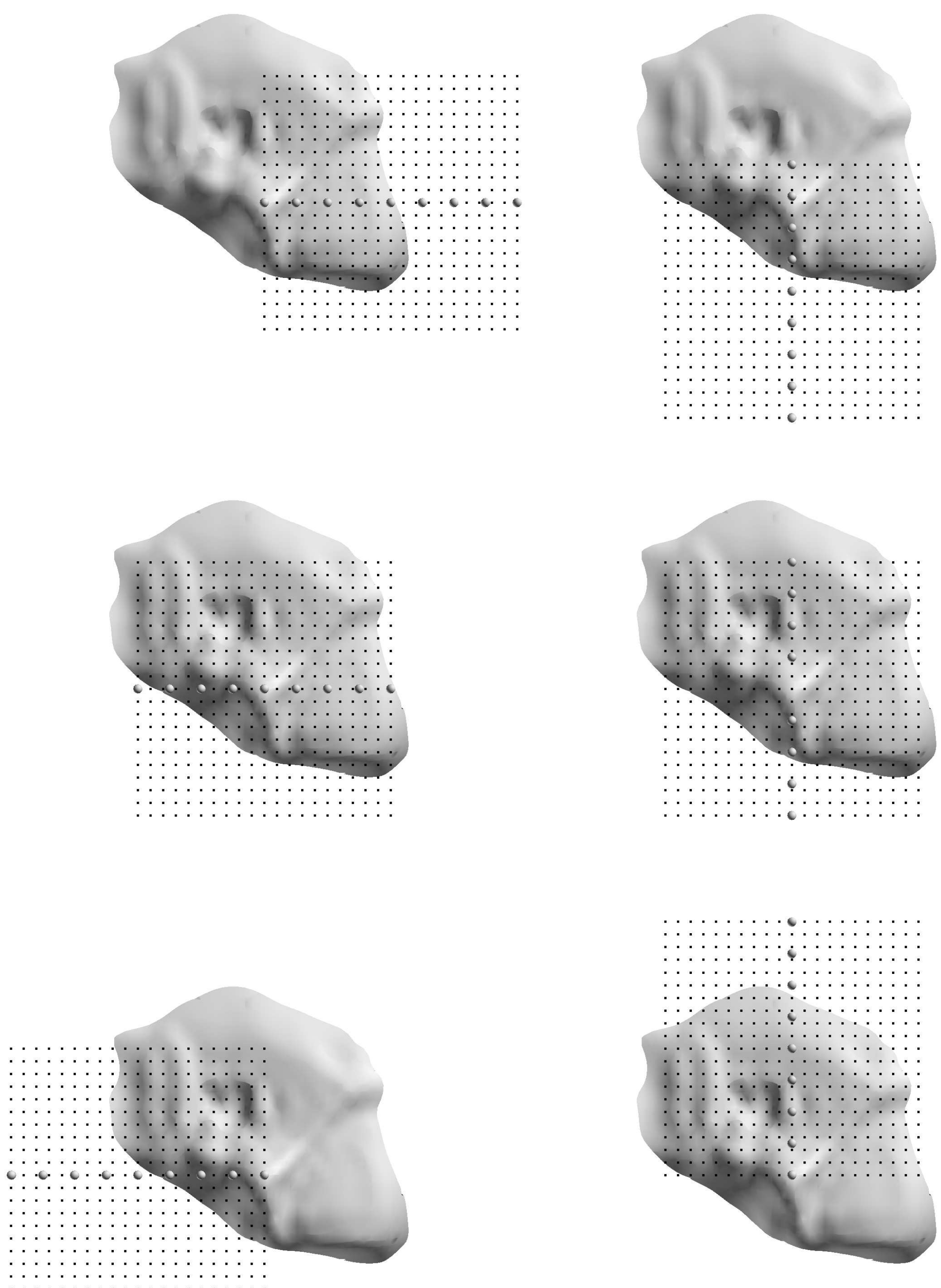

Figure 2. Top view of six shot-receiver configurations M1,...,M6 and the salt body. The spheres represent the shot locations.

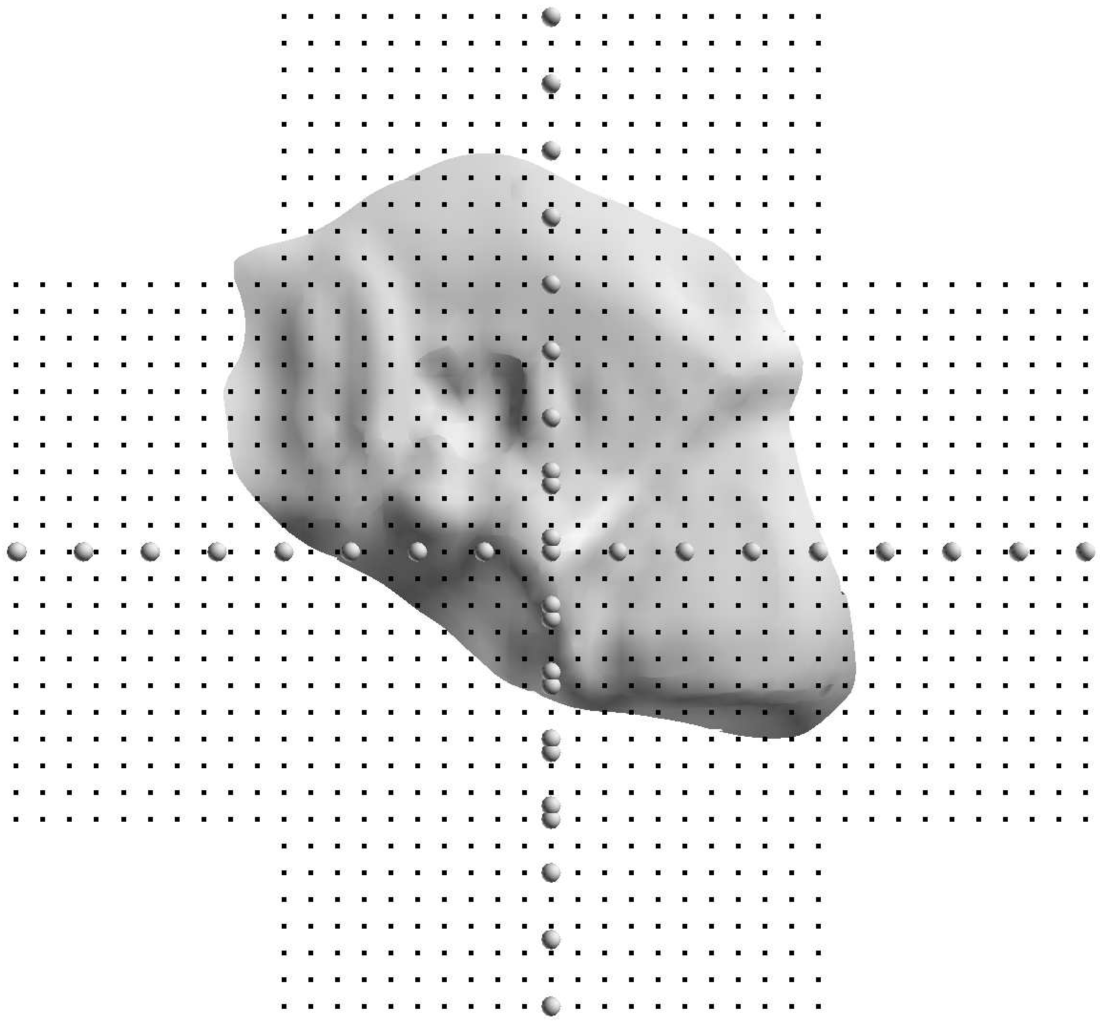

Figure 3. Top view of all shot-receiver configurations M1,...,M6 and the salt body.

4 Ray tracing computations

The two-point rays of reflected P-waves are determined by means of the two-parametric shooting method using the MODEL, CRT and FORMS subroutine packages (Červený, Klimeš & Pšenčík, 1988). The salt model is a complex model and the intersection of the geopressure interface with the salt body required the use of several elementary waves in computing the P-waves reflected from the bottom interface. Twelve elementary waves are defined for each shot. The most time-consuming step of the calculation is the two-point ray tracing. Ray tracing output files are then processed. The rays of the computed waves, maps of the reflection points, shots and receivers are added to the GOCAD files.

Figures 4 and 5 show the two-point rays of selected elementary waves. The figures are screen snapshots of several GOCAD camera positions. A more detailed description of the computation steps can be found in Bucha (2004).

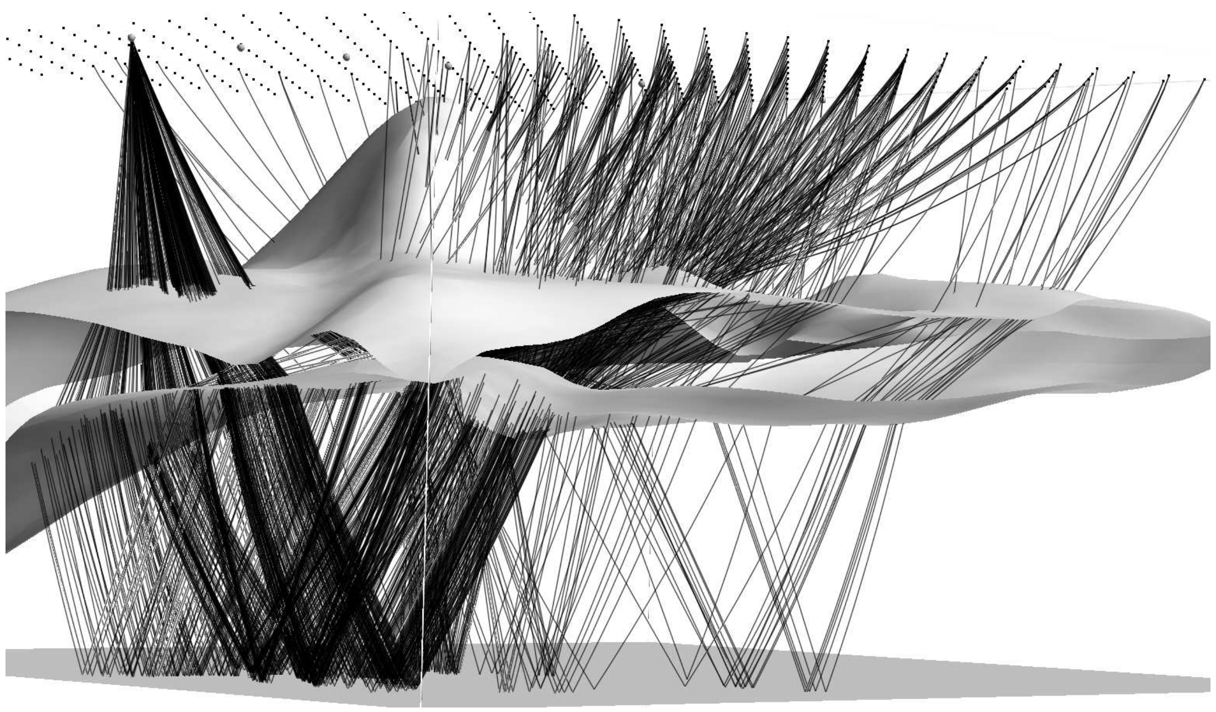

Figure 4. Two-point rays of one elementary P-wave reflected from the bottom flat interface. The model is cut by a GOCAD slicer to show the ray paths in the salt body.

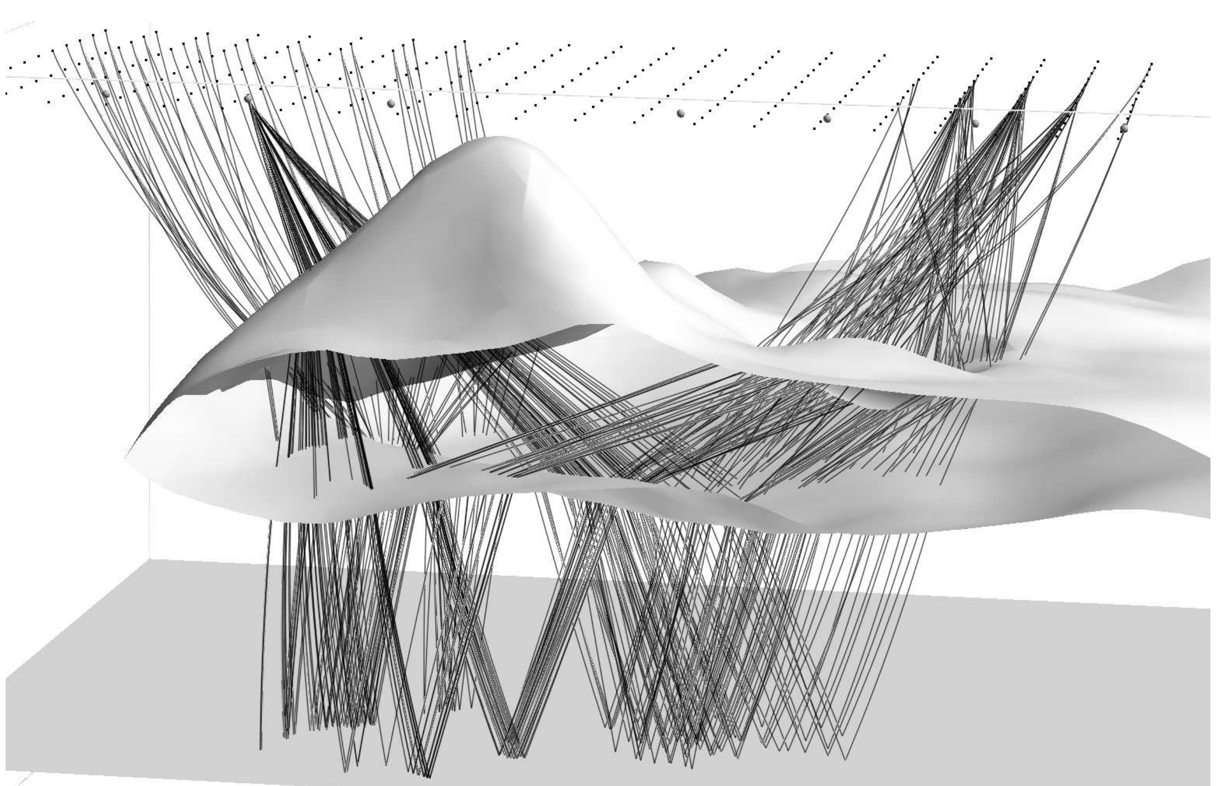

Figure 5. Two-point rays of other elementary P-waves reflected from the bottom flat interface.

5 Maps of reflections

The two-point rays of P-waves reflected from the bottom flat interface for six shot-receiver configurations (53 shots, 2646 receivers) are computed. Figures 6 and 7 show reflection points colour coded according to the reflection amplitude. The distribution and amplitude of the reflection points are affected mainly by the shape of the salt body, by the velocity properties and shot-receiver configuration. The reflection maps show areas of strong and dense reflections below the salt crest and the reflection shadows below the trunk of the salt body, and the trough at the bottom interface of the salt body. The ray paths are in many cases complicated (see Figures 4 and 5), therefore, displaying reflection points and two-point rays for each shot and each elementary wave separately is recommended for detailed studies of subsalt reflections.

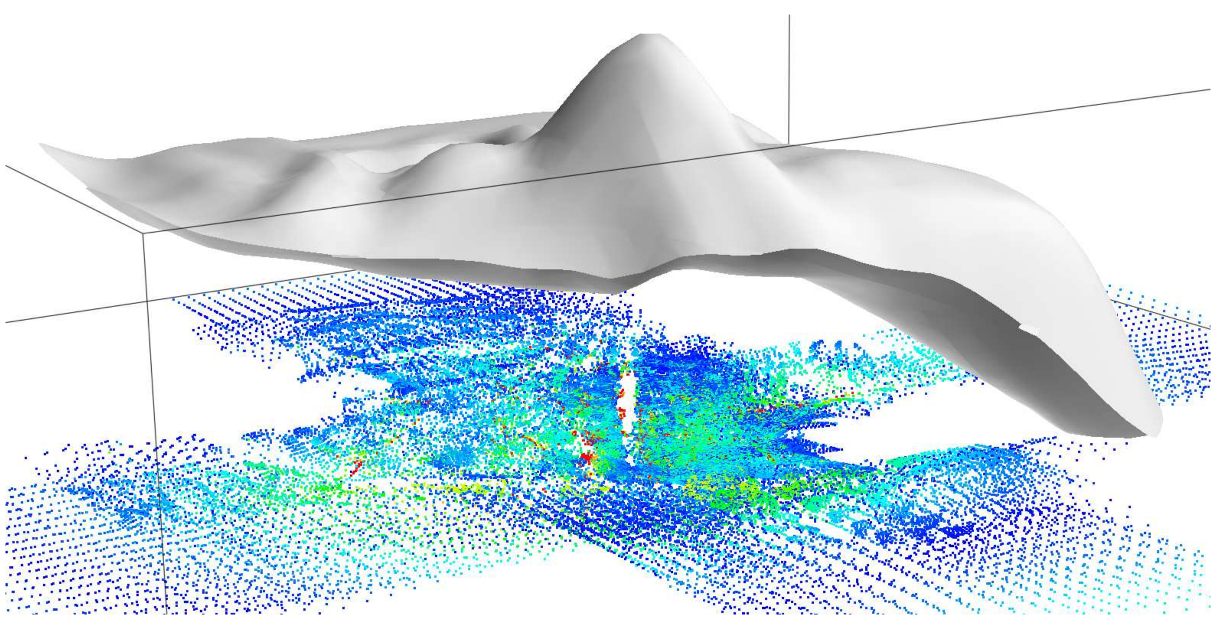

Figure 6. Map of all reflection points for shot-receiver configurations M1,...,M6, colour coded according to amplitude (blue for low amplitude to red for high amplitude).

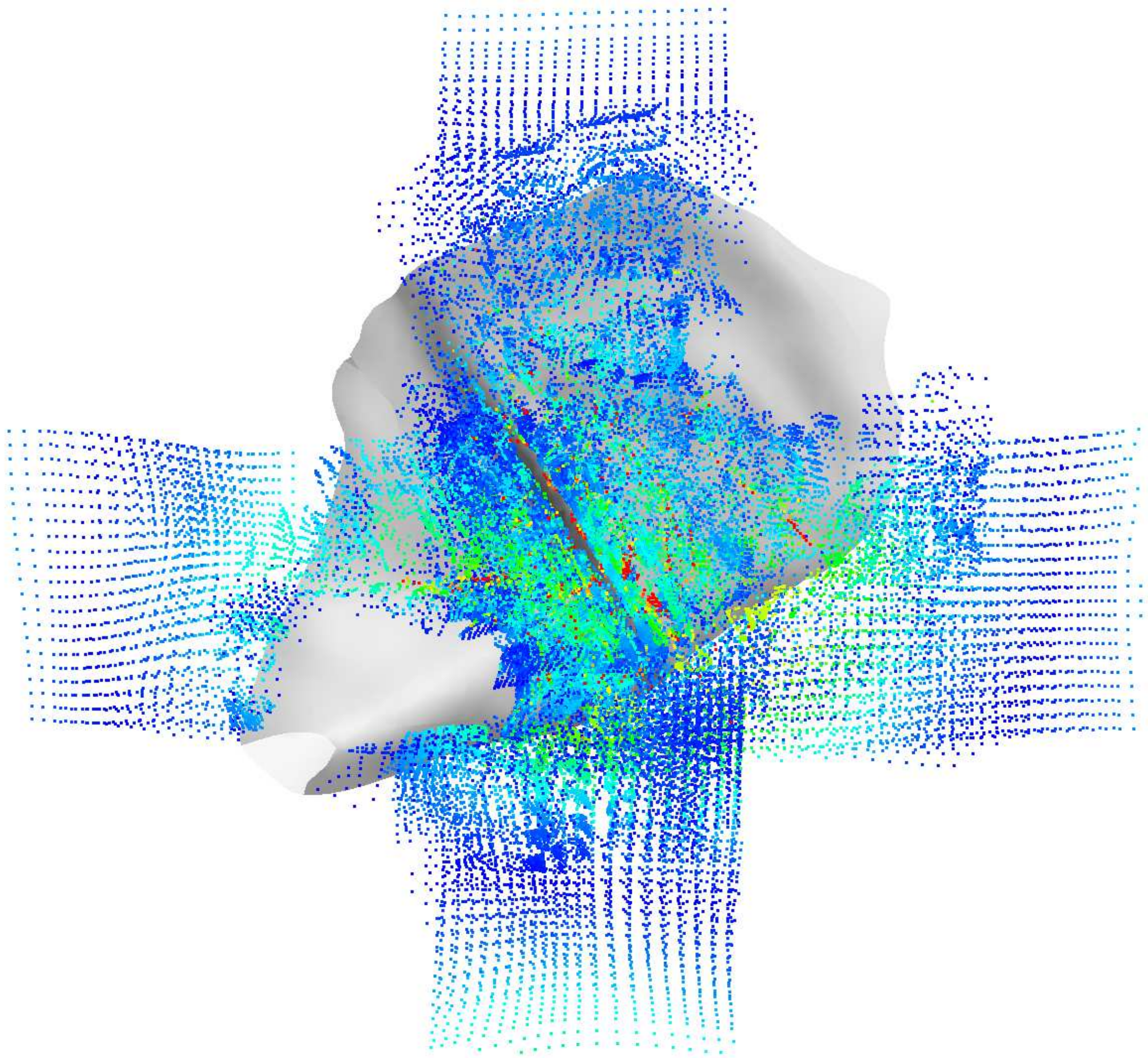

Figure 7. Bottom view of the reflection map for shot-receiver configurations M1,...,M6, colour coded according to amplitude (blue for low amplitude to red for high amplitude).

6 Discussion

How does one illuminate the large shadow below the trunk of the salt body? Two other shot-receiver configurations M7 and M8 (see Figures 8 and 9) were designed and computed. The results of this calculation show that there is no improvement in the illumination of the shadow below the trunk (see Figure 10). Hence one additional test was performed. Twenty-one shots located below the salt body very close to the bottom salt interface were designed. The two-point rays for these twenty-one shots were calculated for the receivers in configurations M1, M4, M7 (see Figures 2 and 8). A simple solution (one or two shots) to illuminate the shadow area below the trunk was not found. Finally eight shots were selected from the initial twenty-one shots (see Figure 11). The map of reflections computed for the selected eight shots illuminates nearly the whole area of the shadow below the trunk (see Figure 12). Figure 13 shows the illumination computed for one shot (two-point rays of one elementary wave for this shot are plotted in Figure 11).

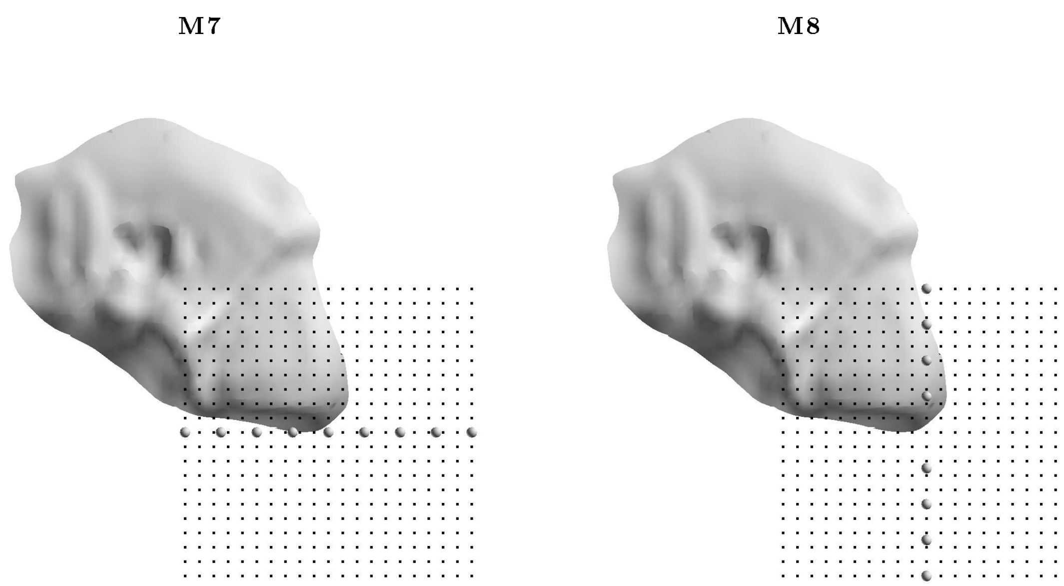

Figure 8. Top view of two shot-receiver configurations M7 and M8 and the salt body. The spheres represent the positions of the shots.

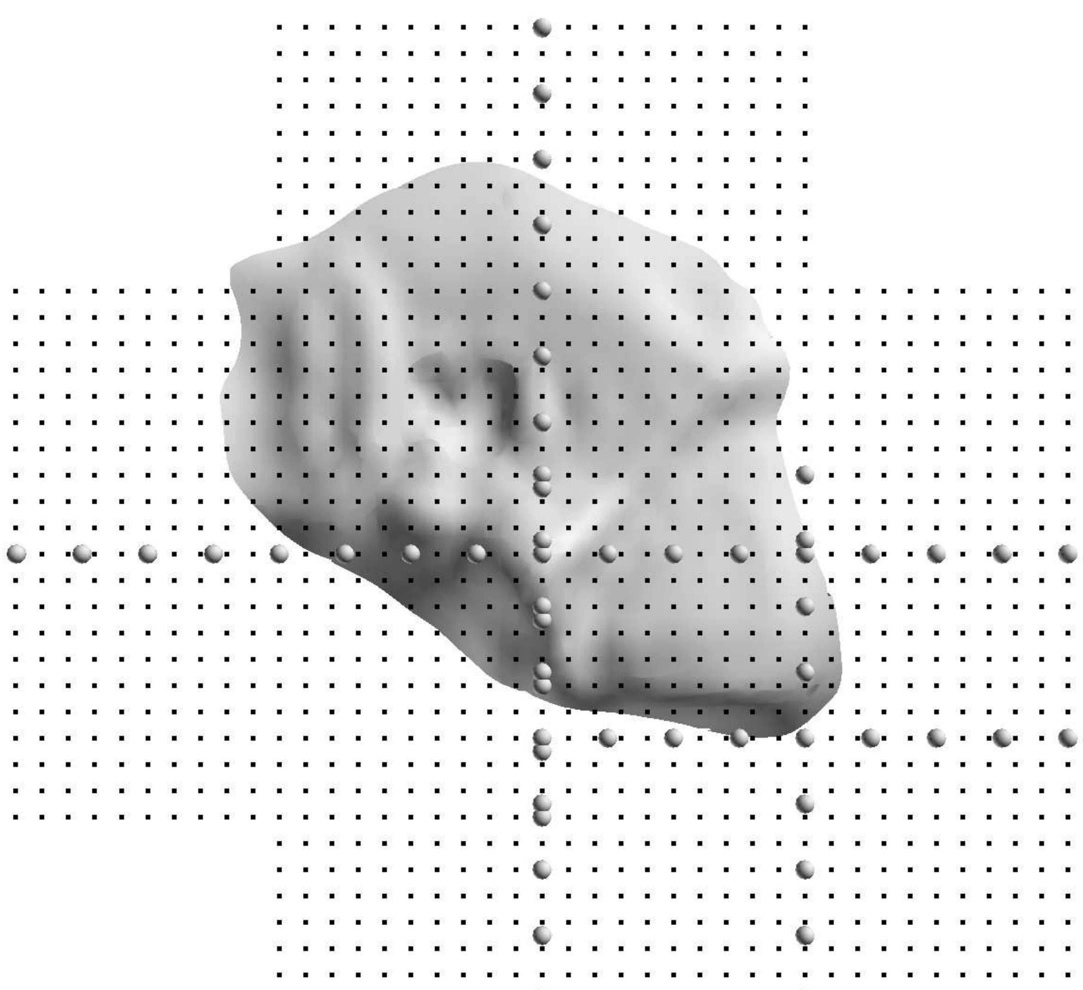

Figure 9. Top view of all shot-receiver configurations M1,...,M8 and the salt body.

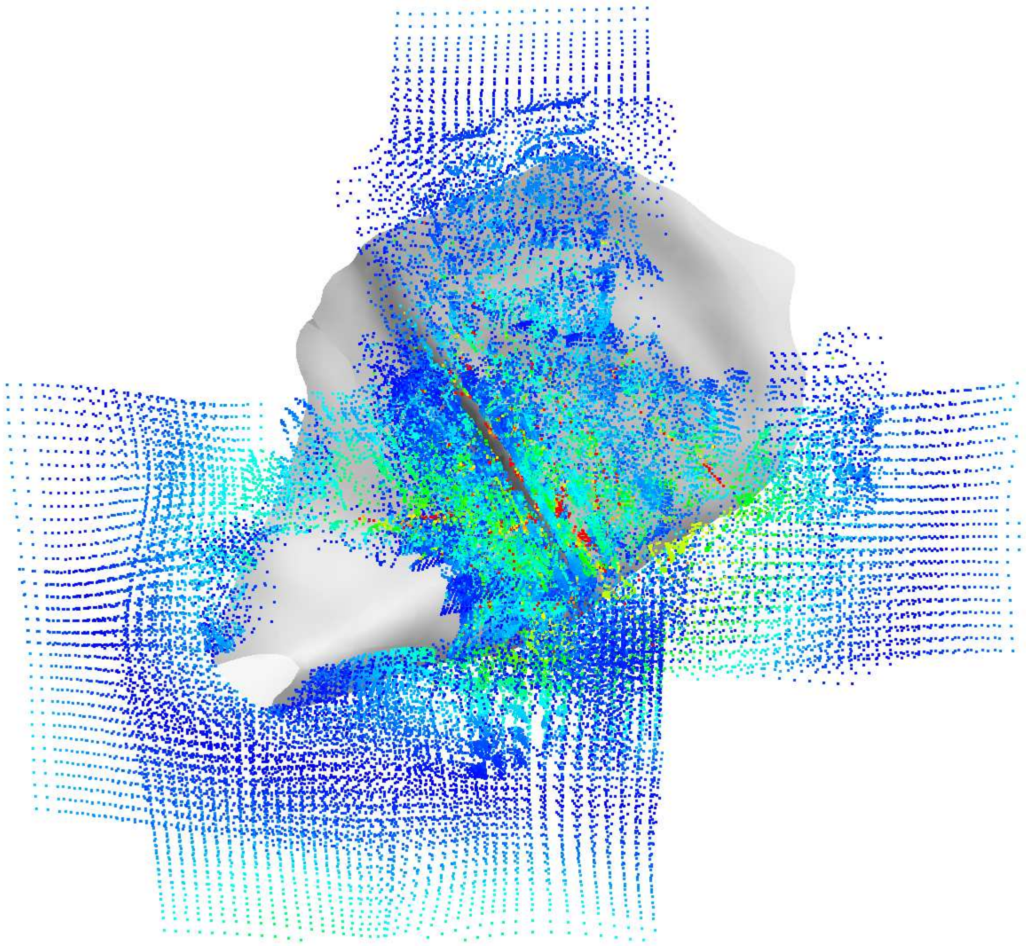

Figure 10. Bottom view of the map of all reflections for shot-receiver configurations M1,...,M8, colour coded according to amplitude (blue for low amplitude to red for high amplitude).

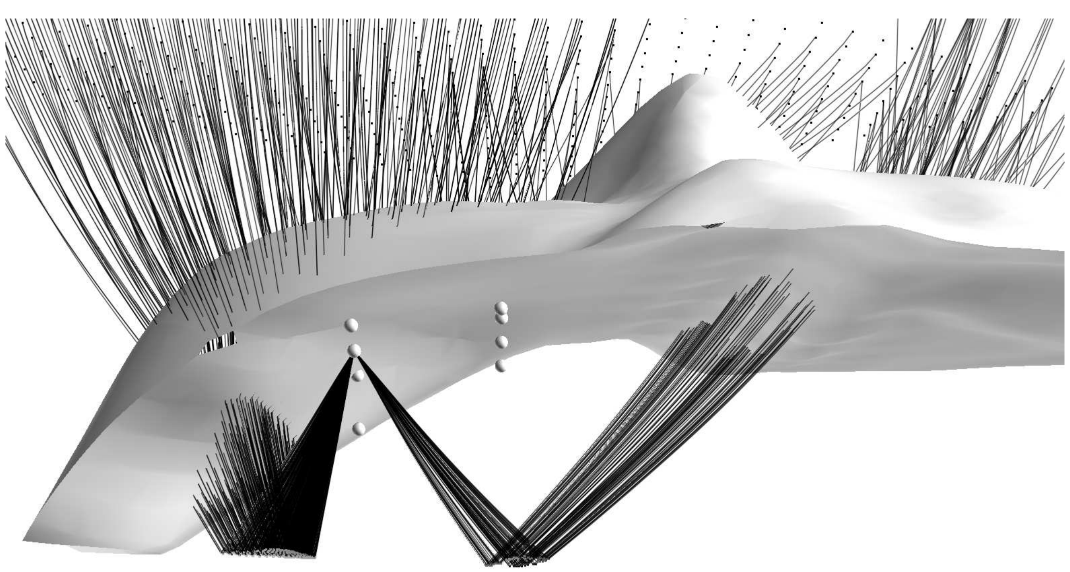

Figure 11. Eight shots under the salt body. Two-point rays of one elementary P-wave reflected from the bottom flat interface.

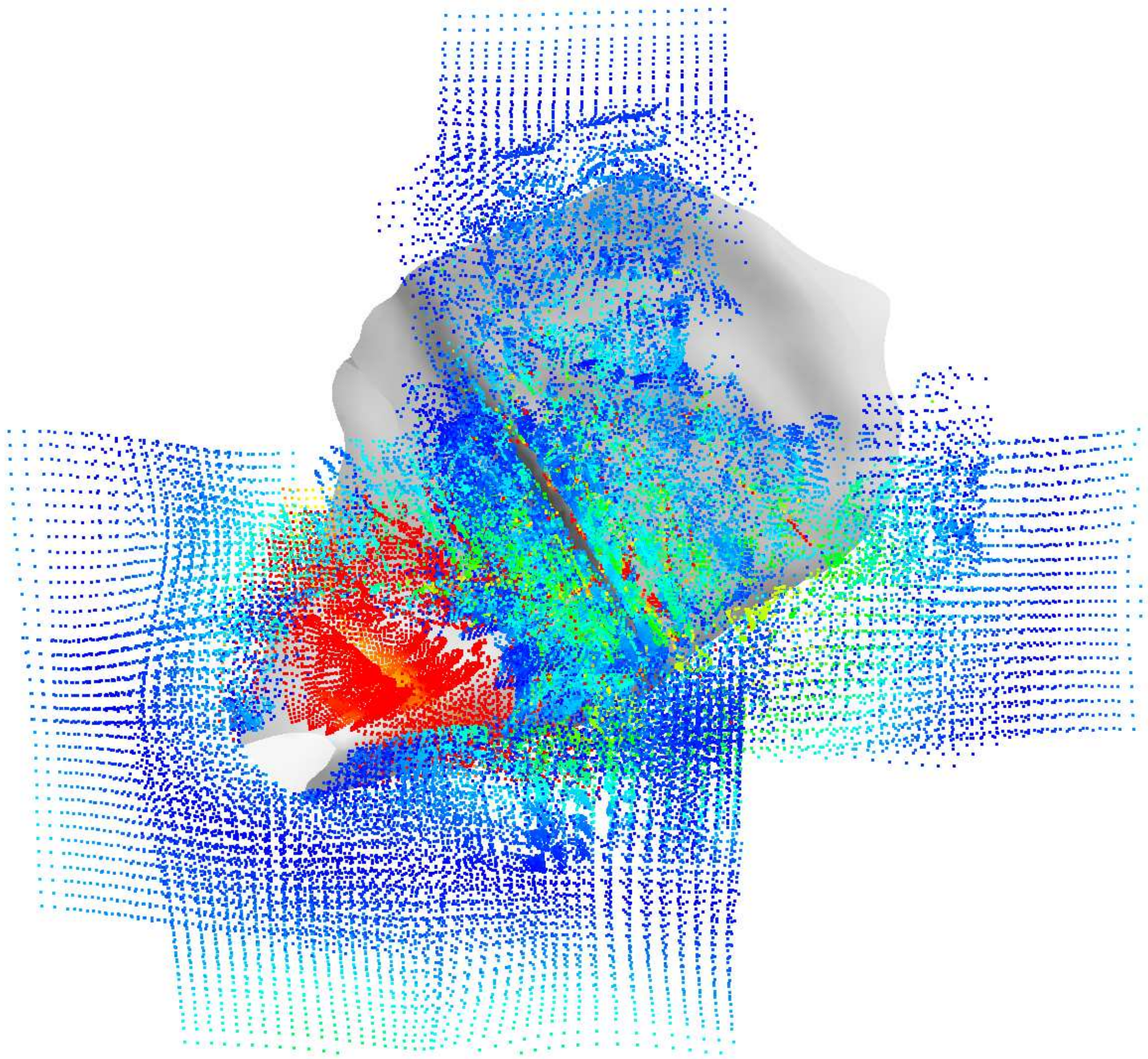

Figure 12. Bottom view of the map of all reflections for shot-receiver configurations M1,...,M8, and eight shots under the salt body (blue for low amplitude to red for high amplitude).

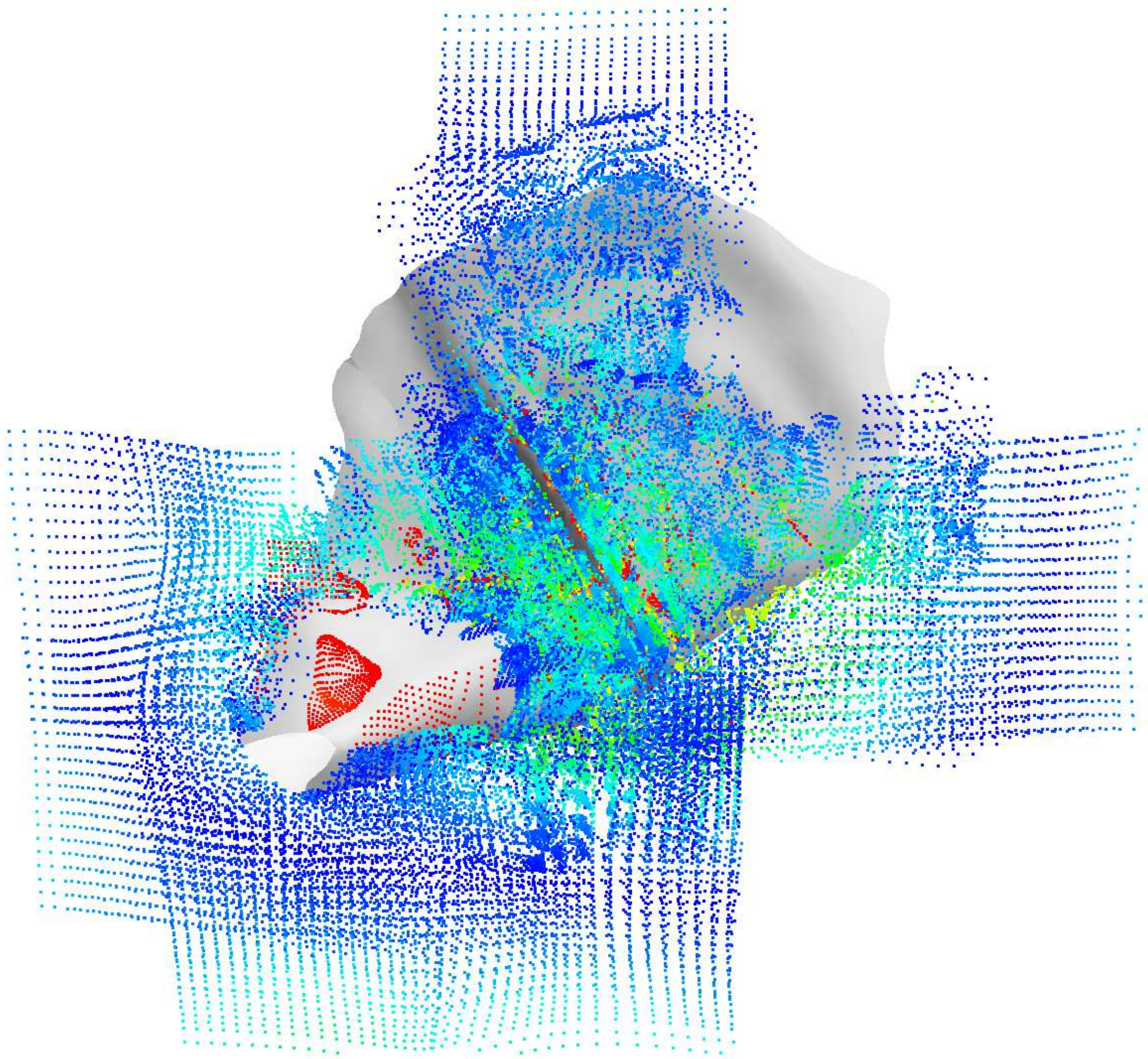

Figure 13. Bottom view of the map of all reflections for shot-receiver configurations M1,...,M8, and one shot under the salt body, colour coded according to amplitude.

7 Conclusions

The results of the calculations show that the smoothed SEG/EAGE Salt Model is suitable for two-point ray tracing. The computation and visualization of rays and maps of reflections of the individual elementary waves is the great advantage of the ray tracing method and should help in studying problems in subsalt areas. The reflection maps on the bottom flat interface show areas with strong and dense reflections and reflection shadows. No simple solution of illuminating the large shadow area below the trunk of the salt body was found.

The average computation time for one shot-receiver configuration (one of M1,...,M8) was approximately 6 hours on a PC equipped with an Athlon 64 3400+ (2.2 GHz) processor and with the Linux operating system.

Acknowledgments

The author thanks Luděk Klimeš for valuable comments and recommendations concerning this paper.

The research was supported by the Grant Agency of the Czech Republic under Contract 205/04/1104, and by the members of the consortium "Seismic Waves in Complex 3-D Structures" (see "http://sw3d.mff.cuni.cz").

References

Aminzadeh, F., Brac, J. & Kunz, T. (1997): 3-D Salt and Overthrust Models. SEG/EAGE 3-D Modeling Series No.1. Soc. Explor. Geophysicists, Tulsa, OK.

Bear, G., Lu, C., Lu, R. & Willen, D. (2000): The construction of subsurface illumination and amplitude maps via ray tracing. The Leading Edge, **19**(7), pp. 726–728.

Bucha, V. (2004): Ray tracing computations in the smoothed SEG/EAGE Salt Model. Part 3: Maps of reflections. In: Seismic Waves in Complex 3-D Structures, Report 14, Dep. Geophys., Charles Univ., Prague, pp. 35–42.

Bucha, V. (2006): Ray tracing computations in the smoothed acoustic SEG/EAGE Salt Model. Part 1: Seismograms. J. Seismic Explor., in press.

Bulant, P. (2001): Sobolev scalar products in the construction of velocity models - application to model Hess, to SEG/EAGE Salt Model, and to model Pluto 1.5. In: Seismic Waves in Complex 3-D Structures, Report 11, pp. 133–159, Dep. Geophys., Charles Univ., Prague.

Bulant, P. (2002): Sobolev scalar products in the construction of velocity models: Application to model Hess and to SEG/EAGE Salt Model. Pure appl. Geophys., **159**, pp. 1487–1506.

Bulant, P. (2004): Constructing the SEG/EAGE 3-D Salt Model for ray tracing using Sobolev scalar products. Stud. Geophys. Geod., **48**, pp. 689–707.

Červený, V., Klimeš, L. & Pšenčík, I. (1988): Complete seismic-ray tracing in three-dimensional structures. In: Doornbos, D.J.(ed.), Seismological Algorithms, Academic Press, New York, pp. 89–168.

Muerdter, D. & Ratcliff, D. (2001a): Understanding subsalt illumination through ray-trace modeling, Part 1: Simple 2-D salt models. The Leading Edge, **20**(6), pp. 578–594.

Muerdter, D., Kelly, M. & Ratcliff, D. (2001b): Understanding subsalt illumination through ray-trace modeling, Part 1: Dipping salt bodies, salt peaks, and nonreciprocity of subsalt amplitude response. The Leading Edge, **20**(7), pp. 688–697.

Muerdter, D. & Ratcliff, D. (2001c): Understanding subsalt illumination through ray-trace modeling, Part 3: Salt ridges and furrows, and the impact of acquisition orientation. The Leading Edge, **20**(8), pp. 803–816.